Inorganic Chemistry
Article

Inorg. Chem. **2010**, *49*, 419–426 **419**
DOI: 10.1021/ic900740n

Chiral Indium Alkoxide Complexes as Initiators for the Stereoselective Ring-Opening Polymerization of *rac*-Lactide

Jean-Charles Buffet,[†] Jun Okuda,[‡] and Polly L. Arnold*[,†]

[†]*School of Chemistry, Joseph Black Building, University of Edinburgh, West Mains Road, Edinburgh, EH9 3JJ, United Kingdom and* [‡]*Institute of Inorganic Chemistry, RWTH Aachen University, Landoltweg 1, D-52074 Aachen, Germany*

Received April 16, 2009

The indium complex InL_2N'' has been prepared from the reaction of 2 equiv of (^{t}Bu)$_2$P(O)CH$_2$CH(^{t}Bu)OH (HL) with InN''_3 (N″ = N(SiMe$_3$)$_2$). This complex reacts with a further equivalent of 2,6-di-*tert*-butylphenol or HL to afford the adducts InL_2(OAr) and InL_3, respectively. Confirmation that the anion L$^-$ exhibits "ligand self-recognition" in the formation of predominantly homochiral complexes *RR*-InL_2N'' and *SS*-InL_2N'' is obtained from ^{1}H and ^{31}P NMR spectroscopic data. However, the self-recognition is less effective at the indium cation, and mixtures of InL_3 complexes with different configurations are observed. Single-crystal X-ray diffraction data confirm the five-coordinate, distorted bipyramidal In center in InL_2N'' and InL_2(OAr) as anticipated. Selected crystals of InL_3 show two of the possible configurations: one is the *fac-RRR*-InL_3 complex, analogous to the lanthanide complexes LnL_3 reported previously (Ln = Y, Eu, Er, Yb); another is the alternative, homochiral mer form *RRR*′-InL_3. All three complexes are efficient single-component initiators for the ring-opening polymerization of *rac*-lactide over a wide range of temperatures and monomer-to-initiator ratios, exhibiting reasonable control over the synthesis of isotactic polylactide. Despite its poorly defined structure, InL_3 is the fastest initiator among the three complexes for the polymerization of *rac*-lactide, and shows the best tacticity control. The polylactide samples have high molecular weights $M_{n,exp}$ (between 44 000 and 270 000 g/mol at completion) and narrow polydispersities (as low as 1.25 at completion).

1. Introduction

Polylactide (PLA) is a biocompatible and biodegradable polyester produced by ring-opening polymerization (ROP) of lactide, a cyclic ester from natural sources. Polylactide possesses versatile physical properties and has been widely used in tissue engineering and in media for the controlled release of drugs.[1−4] ROP of lactide by single-site catalysts is the most efficient route to PLAs with a predicted molecular weight and narrow molecular weight distribution. The past two decades have particularly witnessed the development of initiators for improved polymer stereochemistry, one of the most critical factors in determining the physical and mechanical properties of a polymeric material.[5−8] Catalysts with excellent enantioselective control over the chain initiation and propagation steps have been reported.[9−15]

A wide variety of Al^{III} catalysts, particularly those supported by SALEN- or SALAN-type ancillary ligands, have been demonstrated to show excellent molecular weight and stereochemical control in the ring-opening polymerization

*To whom correspondence should be addressed. Fax: +44 131 650 6453. E-mail: Polly.Arnold@ed.ac.uk.

(1) Platel, R. H.; Hodgson, L. M.; Williams, C. K. *Polym. Rev.* **2008**, *48*, 11–63.
(2) Huang, L.; Zhuang, X.; Hu, J.; Lang, L.; Zhang, P.; Wang, Y.; Chen, X.; Wei, Y.; Jing, X. *Biomacromolecules* **2008**, *9*, 850–858.
(3) Vink, E. T. H.; Rábago, K. R.; Glassner, D. A.; Gruber, P. R. *Polym. Degrad. Stab.* **2003**, *80*, 403–419.
(4) Park, J.; Ye, M.; Park, K. *Molecules* **2005**, *10*, 146–161.
(5) Majerska, K.; Duda, A. *J. Am. Chem. Soc.* **2004**, *126*, 1026–1027.
(6) Hormnirun, P.; Marshall, E. L.; Gibson, V. C.; White, A. J. P.; Williams, D. J. *J. Am. Chem. Soc.* **2004**, *126*, 2688–2689.
(7) Agrawal, A. K.; Bhalla, R. *J. Macromol. Sci., Part C: Polym. Rev.* **2003**, *43*, 479–503.
(8) Numata, K.; Srivastava, R. K.; Finne-Wistrand, A.; Albertsson, A.-C.; Doi, Y.; Abe, H. *Biomacromolecules* **2007**, *8*, 3115–3125.
(9) Wheaton, C. A.; Hayes, P. G.; Ireland, B. J. *Dalton Trans.* **2009**, 4832–4846.
(10) Chisholm, M. H.; Zhou, Z. *J. Mater. Chem.* **2004**, *14*, 3081–3092.
(11) Ma, H.; Okuda, J. *Macromolecules* **2005**, *38*, 2665–2673.
(12) Dechy-Cabaret, O.; Martin-Vaca, B.; Bourissou, D. *Chem. Rev.* **2004**, *104*, 6147–6176.
(13) Simic, V.; Spassky, N.; Hubert-Pfalzgraf, L. G. *Macromolecules* **1997**, *30*, 7338–7340.
(14) O′Keefe, B. J.; Monnier, S. M.; Hillmyer, M. A.; Tolman, W. B. *J. Am. Chem. Soc.* **2001**, *123*, 339–340.
(15) Save, M.; Schappacher, M.; Soum, A. *Macromol. Chem. Phys.* **2002**, *203*, 889–899.

Published on Web 12/14/2009

Chart 1

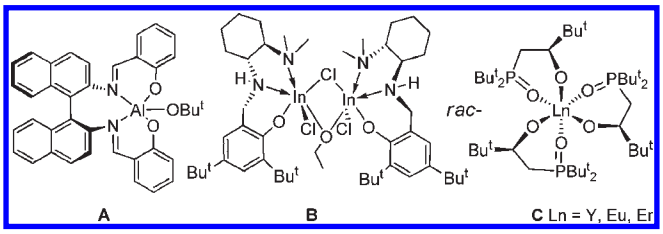

of lactide, such as **A** (see Chart 1).[16−27] However, from the rest of the complexes of group 13 metals, there are only two reported examples to date of a well-defined indium complex; **B** catalyzes the ROP of *rac*-lactide in a living manner, showing modest isoselectivity.[28,29] It has recently been shown that simple mixtures of indium trichloride, benzyl alcohol, and triethylamine catalyze the ROP of *rac*-lactide to form highly heterotactic polylactide,[30] and indium complexes have previously shown some potential as ROP initiators of ε-caprolactone polymerization.[31]

We previously reported that a racemic mixture of a bidentate proligand *rac*-HL, which contains a single stereogenic center, is resolved into a mixture of two homochiral C_3-symmetric complexes for the first time upon lanthanide complexation to form *RRR*-LnL_3 and *SSS*-LnL_3, **C**.[32] The resolution affords about 80% of the product as a homochiral tris(L) complex, while the remaining 20% comprised diastereomers *RRS*-LnL_3 and *SSR*-LnL_3. The utility of ligand self-recognition[33,34] was demonstrated by the use of these chiral complexes as initiators for the formation of isotactic polylactide. More recently, we have shown that the bis(L) adduct YL_2N'' can be isolated from the reaction of YN''_3 with *rac*-HL ($N'' = N(SiMe_3)_2$), but with a less efficient resolution: 65% of the product is homochiral *RR*- and *SS*-YL_2N'' and 35% is *RS*-YL_2N''.[35] As indium is a Lewis-acidic, trivalent metal with a smaller ionic radius than Y ($r(In^{3+}) = 0.800$ Å, $r(Y^{3+}) = 0.900$ Å),[36,37] and a preference for five-coordinate geometries,[38] it was deemed that better resolution with L would result. It is generally regarded that indium metal is not toxic, but the toxicity of indium compounds has not yet been thoroughly investigated, so it is not clear yet how it compares to yttrium and lanthanide salts, which are regarded as nontoxic by ingestion.[39] Herein, we report the synthesis and characterization of chiral indium complexes InL_2N'' (**1**), $InL_2(OAr)$ (**2**), and InL_3 (**3**) along with their molecular structures and activity in *rac*-lactide polymerization.

2. Experimental Section

2.1. General Details. All manipulations were carried out using standard Schlenk techniques, or a Vacuum Atmosphere double glovebox, under an atmosphere of dry nitrogen. Pentane, hexane, toluene, diethyl ether, and THF were dried by passage through activated alumina towers and degassed before use. DME was distilled from potassium under an atmosphere of dry nitrogen. All solvents were stored over potassium mirrors (with the exception of THF and DME, which were stored over activated 4 Å molecular sieves). Deuterated solvents were distilled from potassium, degassed by three freeze−pump−thaw cycles, and stored under nitrogen.

The epoxide 3,3-dimethyl-epoxybutane, purchased from Alfa Aesar, was distilled and stored over activated molecular sieves prior to use, *rac*-lactide was purchased from Alfa Aesar, recrystallized from hot toluene, washed with diethyl ether, and sublimed (10^{-4} torr, 110 °C) prior to use. 2,6-Di-*tert*-butylphenol, purchased from Aldrich, was sublimed (10^{-4} Torr, 80 °C) prior to use. The compounds $(^tBu)_2P(O)CH_2CH(^tBu)OH$ (HL), and the enantiopure form *R*-HL,[32] and $In[N(SiMe_3)_2]_3$ (InN''_3)[40] were made according to literature procedures.

NMR spectra (^1H, $^{13}C\{^1H\}$, and $^{31}P\{^1H\}$) were recorded at 298 K on a Bruker DRX 400 spectrometer, with an operating frequency at 400.1 MHz (^1H), 100.6 MHz (^{13}C), and 161.9 (^{31}P), or on a Bruker ARX 250, DPX 360, or DMX 500, operating at 250.1, 360.1, or 500.1 (^1H); 63.0, 90.7, or 126.0 (^{13}C); and 101.3, 145.8, or 202.47 (^{31}P) MHz, respectively. Chemical shifts are quoted in parts per million and are relative to external $SiMe_4$ or H_3PO_4. Benzene-d_6 and toluene-d_8 were purchased from Aldrich and distilled from potassium. Elemental microanalyses were carried out by Mr. Stephen Boyer at the Microanalysis Service, London Metropolitan University, United Kingdom. Polymer molecular weight and molecular weight distributions were obtained using a Gel Permeation Chromatography PLgel 5 μm Mixed-C column (300 × 7.5 mm) from Polymer Laboratories on an Agilent 1100 HPLC. Data were analyzed using ChemStation software. Polymer analysis was run using THF as the eluent at a flow rate of 0.5 mL/min at 35 °C. The polymer was detected using a RID detector. Polystyrenes (Polymer Laboratories) with a peak molecular weight range from 580 to 300 000 g/mol were used as standards.

2.2. Synthesis of Complexes. Synthesis of InL_2N'' (1). To a solution of 1 equiv of InN''_3 in THF (100.0 mg, 0.17 mmol, 2 mL) was added a solution of 2 equiv of HL in THF (89.1 mg,

(16) Du, H.; Velders, A. H.; Dijkstra, P. J.; Zhong, Z.; Chen, X.; Feijen, J. *Macromolecules* **2009**, *42*, 1058–1066.
(17) Chisholm, M. H.; Gallucci, J. C.; Quisenberry, K. T.; Zhou, Z. *Inorg. Chem.* **2008**, *47*, 2613–2624.
(18) Iwasa, N.; Fujiki, M.; Nomura, K. *J. Mol. Catal. A: Chem.* **2008**, *292*, 67–75.
(19) Tang, Z.; Gibson, V. C. *Eur. Polym. J.* **2007**, *43*, 150–155.
(20) Lian, B.; Thomas, C. M.; Casagrande, O. L.; Lehmann, C. W.; Roisnel, T.; Carpentier, J.-F. *Inorg. Chem.* **2007**, *46*, 328–340.
(21) Zhong, Z.; Dijkstra, P. J.; Feijen, J. *Angew. Chem., Int. Ed.* **2002**, *41*, 4510–4513.
(22) Chisholm, M. H.; Patmore, N. J.; Zhou, Z. *Chem. Commun.* **2005**, 127–129.
(23) Yang, J.; Yu, Y.; Li, Q.; Li, Y.; Cao, A. *J. Polym Sci., Part A: Polym. Chem.* **2005**, *43*, 373–384.
(24) Wisniewski, M.; Le Borgne, A.; Spassky, N. *Macromol. Chem. Phys.* **1997**, *198*, 1227–1238.
(25) Spassky, N.; Wisniewski, M.; Pluta, C.; Le Borgne, A. *Macromol. Chem. Phys.* **1996**, *197*, 2627–2637.
(26) Ovitt, T. M.; Coates, G. W. *J. Am. Chem. Soc.* **2002**, *124*, 1316–1326.
(27) Radano, C. P.; Baker, G. L.; Smith, M. R. *J. Am. Chem. Soc.* **2000**, *122*, 1552–1553.
(28) Douglas, A. F.; Patrick, B. O.; Mehrkhodavandi, P. *Angew. Chem., Int. Ed.* **2008**, *47*, 2290–2293.
(29) Peckermann, I.; Kapelski, A.; Spaniol, T. P.; Okuda, J. *Inorg. Chem.* **2009**, *48*, 5526–5534.
(30) Pietrangelo, A.; Hillmyer, M. A.; Tolman, W. B. *Chem. Commun.* **2009**, 2736–2737.
(31) Hsieh, I. P.; Huang, C.-H.; Lee, H. M.; Kuo, P.-C.; Huang, J.-H.; Lee, H.-I.; Cheng, J.-T.; Lee, G.-H. *Inorg. Chim. Acta* **2006**, *359*, 497–504.
(32) Arnold, P. L.; Buffet, J.-C.; Blaudeck, R. P.; Sujecki, S.; Blake, A. J.; Wilson, C. *Angew. Chem., Int. Ed.* **2008**, *47*, 6033–6036.
(33) Masood, M. A.; Eric, J. E.; Stack, T. D. P. *Angew. Chem., Int. Ed.* **1998**, *37*, 928–932.
(34) Seeber, G.; Tiedemann, B. E. F.; Raymond, K. N. *Top. Curr. Chem.* **2006**, *265*, 147–183.
(35) Arnold, P. L.; Buffet, J.-C.; Blaudeck, R. P.; Sujecki, S.; Wilson, C. *Chem.—Eur. J.* **2009**, *15*, 8241–8250.
(36) Peckermann, I.; Robert, D.; Englert, U.; Spaniol, T. P.; Okuda, J. *Organometallics* **2008**, *27*, 4817–4820.
(37) Shannon, R. D. *Acta Crystallogr., Sect. A* **1976**, *32*, 751–767.
(38) Atwood, D. A.; Hutchison, A. R.; Zhang, Y. *Struct. Bonding (Berlin, Ger.)* **2003**, *105*, 167−201.
(39) Hayes, A. W. *Principles and Methods of Toxicology*; 5th ed.; Taylor and Francis: Philadelphia, 2007; pp 2270.
(40) Bürger, H.; Cichon, J.; Goetze, U.; Wannagat, U.; Wismar, H. J. *J. Organomet. Chem.* **1971**, *33*, 1–12.

0.34 mmol, 2 mL) at 25 °C, which was stirred overnight. Volatiles were removed under reduced pressure and the residual solid recrystallized from hexane to afford colorless **1**. Yield: 96 mg (70%). The pure *RR*- diastereomer **1a** was also made in a separate reaction using the above procedure with racemic HL replaced by enantiopure *R*-HL.

^{1}H NMR $\delta(C_6D_6)$: 0.62 (s, 18 H, CH_3), 1.12 (d, 18 H, $^2J_{PC}$ = 13.1 Hz, P-^{t}Bu), 1.16 (s, 18 H, C-^{t}Bu), 1.22 (d, 18 H, $^2J_{PC}$ = 13.2 Hz, P-^{t}Bu), 1.7−1.9 (m, 4 H, CH_2), 4.37 (m, 2 H, CH). ^{13}C{^{1}H} NMR $\delta(C_6D_6)$: 6.6 (6 C, s, $SiMe_3$), 24.0 (2 C, d, J_{PC} = 57.2 Hz, CH_2), 26.6 (6 C, s, CMe_3), 27.0 (6 C, s, P-CMe_3), 27.1 (6 C, s, P-CMe_3), 79.4 (2 C, d, $^2J_{PC}$ = 6.1 Hz, C−OH). ^{31}P{^{1}H} NMR $\delta(C_6D_6)$: 83.8. Anal. Found: C, 51.14%; H, 9.75%; N, 1.83%. Calcd: C, 51.18%; H, 9.85%; N, 1.76%. FTIR (nujol cm^{-1}): 2730 (w) 1309 (w), 1266 (m), 1104 (s, P═O coordinated), 1025 (m), 896 (w), 807 (w), 728 (w).

Synthesis of InL$_2$(OAr) (2). To a solution of **1** in C_6D_6 (100.0 mg, 0.125 mmol, 2 mL) was added a solution of 2,6-di-*tert*-butylphenol (25.8 mg, 0.125 mmol, 2 mL) at 25 °C, and the mixture was then heated for 16 h at 80 °C. Volatiles were removed under reduced pressure. The residual solid was washed with hexane and dissolved in DME. Then, the solution was evaporated slowly, to afford colorless **2**. Yield: 80.2 mg (76.4%). The pure *RR*-diastereomer **2a** was also made in a separate reaction using the above procedure with racemic HL replaced by enantiopure *R*-HL.

^{1}H NMR $\delta(C_6D_6)$: 0.94 (d, 18 H, $^2J_{PC}$ = 13.7 Hz, P-^{t}Bu), 1.14 (d, 18 H, $^2J_{PC}$ = 13.5 Hz, P-^{t}Bu), 1.15 (s, 18 H, C-^{t}Bu), 1.90. (s, 18 H, Ph-^{t}Bu), 1.7−1.9 (m, 4 H, CH_2), 4.41 (m, 2 H, CH); 6.88 (t, 1 H, p-Ph), 7.44 (d, 2 H, H-meta). ^{13}C{^{1}H} NMR $\delta(C_6D_6)$: 33.1 (6 C, s, ^{t}Bu), 79.3 (2 C, s, C−OH), 115.62 (1 C, p-Ph), 125.98 (2 C, m-Ph), 141.0 (2 C, o-Ph), 166.9 (1 C, C−O). ^{31}P{^{1}H} NMR $\delta(C_6D_6)$: 72.94. Anal. Found: C, 59.92%; H, 9.61%. Calcd: C, 59.85%; H, 9.69%.

Synthesis of InL$_3$ (3). To a solution of InN″$_3$ in THF (100 mg, 0.17 mmol, 2 mL) was added a THF solution of HL (132 mg, 0.50 mmol, 2 mL) at 25 °C, and the mixture heated for 7 days at 80 °C. Volatiles were removed under reduced pressure and the residual solid recrystallized from DME to afford colorless **3**. The complex isolated was analyzed by NMR spectroscopy to be a mixture of isomers. Yield: 70.9 mg (47.0%).

^{1}H NMR $\delta(C_6D_6)$: 1.15−1.4 (complex mixture, 57 H, P^{t}Bu and C^{t}Bu), 1.7−1.9 (m, 6 H, CH_2), 4.4−4.8 (m, 3 H, CH). ^{31}P{^{1}H} NMR $\delta(C_6D_6)$: 65.6 (0.5), 68.6 (0.36), 69.4 (1.0) [relative intensities in brackets]. Anal. Found: C, 56.07%; H, 10.00%. Calcd: C, 56.12%; H, 10.09%.

IR data (nujol, cm^{-1}): 2730 (w), 1357 (m), 1236 (m), 1211 (m), 1186 (m), 1106 (s, P═O coordinated), 1065 (s, P═O uncoordinated), 1016 (s), 961 (s), 823 (m), 643 (m).

IR data (toluene solution, cm^{-1}): 2585 (m), 1942 (m), 1802 (m), 1605 (m), 1455 (m), 1249 (s), 1212 (s), 1178 (s), 1107 (s, P═O coordinated), 1077 (s, P═O uncoordinated), 1040 (s), 966 (m), 931 (m), 895 (m), 842 (s), 784 (s).

2.3. X-Ray Crystallographic Structure Determination for Complexes 1, 2, and 3. Single crystals of **1**, **2**, and three different samples of **3** were mounted on a glass fiber and transferred to a Bruker SMART APEX CCD diffractometer[41] equipped with a graphite-monochromated Mo Kα radiation source (λ = 0.71073 Å) and ω scan measurement. Data were integrated using SAINT, and absorption correction was performed with the program SADABS. Structure solution and refinement was carried out using the SIR 92 program,[42] WinGX,[43] and the SHELXTL[44] suite of programs, and graphics were generated using Ortep.[45] All non-hydrogen atoms were refined with anisotropic thermal parameters. Hydrogen atoms were placed using a "riding model". Details are given in Table 1.

Single crystals of **1** were grown from a cooled hexane solution; single crystals of **2** and **3′** were grown via evaporation of a DME solution, and single crystals of **3** were grown from a cooled hexane/DME solution.

2.4. Lactide Polymerization. General procedure: a Schlenk flask was charged with *rac*-lactide (500 mg, 3.47 mmol), which was dissolved in the volume of solvent required (to give the ratio in the table entry), and the solution was stirred at a desired temperature (given in the table). To this was added a solution of initiator (**1** to **3**) in a solvent via cannula (details given in each table entry). Aliquots were removed via syringe and quenched/precipitated with MeOH (after the time stated in the table). The obtained polymer was dissolved in dichloromethane, filtered through silica gel 60, and dried. The yield for each completed polymerization was quantitative.

3. Results and Discussion

3.1. Synthesis of Complexes *rac*-InL$_2$N″, 1; *rac*-InL$_2$(OAr), 2; and *rac*-InL$_3$, 3. A reaction mixture of InN″$_3$ and 2 equiv of HL at −78 °C was allowed to warm to room temperature and worked up after 16 h to afford diastereomers of the complex **1**, *rac*-InL$_2$N″ (eq 1).

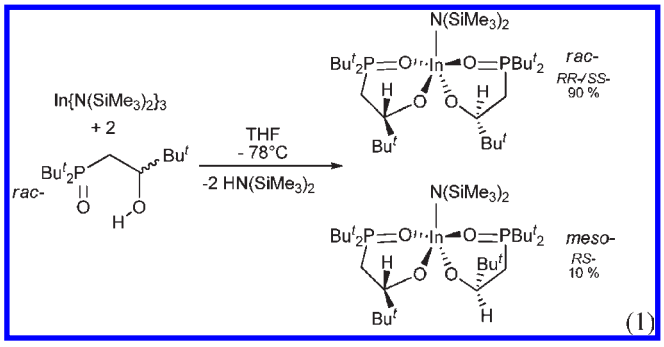

Enantiopure *R*-HL was also used in the synthesis of diastereomerically pure InL$_2$N″ (i.e., *RR*-InL$_2$N″, **1a**). The ^{1}H and ^{31}P{^{1}H} NMR spectra of solutions of **1a** show a single ligand environment for *RR*-InL$_2$N″ (see the Supporting Information, Figure SI 1). NMR spectra of solutions of **1** show the same resonances assigned as the homochiral isomers *RR*-InL$_2$N″ and *SS*-InL$_2$N″, this component of the mixture comprising approximately 90% of the product. The remaining 10% of the total yield is the meso diastereoisomer *RS*-InL$_2$N″, although the resonances are difficult to integrate since they overlap with those of the bulk homochiral product.

Heating a mixture of InL$_2$N″ and 1 equiv of 2,6-di-*tert*-butylphenol at 80 °C for 16 h afforded the complex *rac*-InL$_2$(OAr) **2** (Ar = C_6H_3-Bu^t-2,6) (eq 2) after workup.

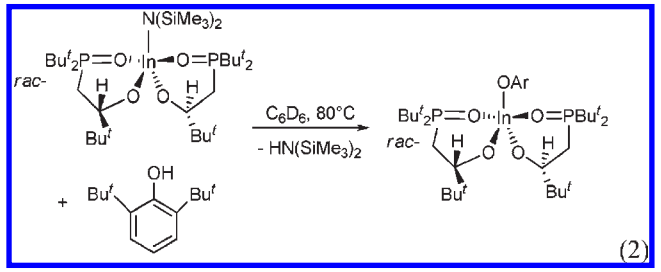

The ^{1}H and ^{31}P{^{1}H} NMR spectra of **2** in benzene-d_6 at room temperature display a single set of resonances for

(41) From Bruker AXS, Madison, WI, 2001.
(42) Altomare, A.; Cascarano, G.; Giacovazzo, C.; Guagliardi, A.; Burla, M. C.; Polidori, G.; Camalli, M. *J. Appl. Crystallogr.* **1994**, *27*, 435.
(43) Farrugia, L. *J. Appl. Crystallogr.* **1999**, *32*, 837−838.
(44) Sheldrick, G. *Acta Crystallogr., Sect. A* **2008**, *64*, 112−122.
(45) Farrugia, L. *J. Appl. Crystallogr.* **1997**, *30*, 565.

Table 1. Experimental Crystallographic Data for Complexes **1**−**3**[a]

compound	InL_2N'', **1**	$InL_2(OAr)$, **2**	InL_3, **3**	InL_3', **3′**
empirical formula	$C_{34}H_{78}In_1N_1O_4P_2Si_2$	$C_{42}H_{81}InO_5P_2$	$C_{42}H_{90}InO_6P_3.C_4H_{10}O_2$	$C_{42}H_{90}InO_6P_3$
M_r	797.91	842.83	988.99	898.87
cell setting	monoclinic	orthorhombic	tetragonal	monoclinic
cryst syst	*P*12/*n*1	*P*212121	$P4_3$	*P*121/*c*1
a, *b*, *c* (Å)	13.5420 (7), 10.9614 (6), 14.4927 (8)	10.5951 (2), 18.1438 (4), 24.2262 (5)	12.5537 (18), 12.5537 (18), 35.309 (7)	19.2795 (5), 12.5166 (3), 21.7618 (5)
α, β, γ (deg)	90.000 (0), 92.340 (2), 90.000 (0)	90.00, 90.00, 90.00	90.00, 90.00, 90.00	90.00, 105.110 (1), 90.00
V (Å^3)	2149.49 (3)	4657.13 (2)	5564.6 (16)	5069.87 (14)
Z	2	4	4	4
D_{calcd} (Mg m^{-3})	1.23	1.20	1.181	1.18
μ (mm^{-1})	0.713	0.614	0.55	0.599
cryst form	prism	block	prism	prism
color	colorless	colorless	colorless	colorless
cryst size (mm)	0.53 × 0.33 × 0.18	0.35 × 0.32 × 0.21	0.20 × 0.10 × 0.03	0.65 × 0.40 × 0.25
T (°C)	−150 (2)	−150 (1)	−178 (2)	−150 (1)
F(000)	855.9	1807.8	2135.8	1935.8
data collection	SMART (Siemens, 1993)	SMART (Siemens, 1993)	dtprofit.ref	SMART (Siemens, 1993)
diffractometer	Bruker Smart Apex CCD area detector	Bruker Smart Apex CCD area detector	Bruker SMART APEX CCD area detector	Bruker Smart Apex CCD area detector
absorption correction	multiscan	multiscan	multiscan	multiscan
T_{min}	0.6314	0.6283	0.766	0.6087
T_{max}	0.7461	0.7461	1.000	0.7461
no. of measured, independent, obsd reflns	25829, 6157, 5864	47190, 13576, 12674	24372, 7628, 5615	76637, 14888, 47190
criterion for obsd reflns	$I > 2\sigma(I)$	$I > 2\sigma(I)$	$I > 2\sigma(I)$	$I > 2\sigma(I)$
R_{int}	0.036	0.041	0.152	0.047
R_{merge}	0.031	0.050	0.152	0.044
θ_{max} (deg)	30.5	30.5	23.3	30.5
$R[F^2 > 2\sigma(F^2)]$, $wR(F^2)$, *S*	0.0391, 0.0844, 1.181	0.0557, 0.1128, 1.167	0.091, 0.287, 1.04	0.0555, 0.0465, 1.164
no. of reflns	6157	13576	7628	14888
no. of params	234	475	495	517
H-atom treatment	riding	riding	riding	riding
weighting scheme	calculated	calculated	calculated	calculated
$\Delta\rho_{max}$, $\Delta\rho_{min}$ (e Å^{-3})	+1.146, −0.732	+1.020, −0.729	+1.16, −1.43	+2.115, −0.667
absolute structure	Flack H D (1983), Acta Cryst. A39, 876−881	Flack H D (1983), Acta Cryst. A39, 876−881	Flack H D (1983), Acta Cryst. A39, 876−881	Flack H D (1983), Acta Cryst. A39, 876−881
Flack parameter		0.492 (19)	0.95 (6)	

[a] Computer programs: Bruker SMART version 5.624 and 5.625 (Bruker, 2001); Bruker SAINT version 6.36a (Bruker, 2002); Bruker SHELXTL (Bruker, 2001); SHELXL-97 (Sheldrick, 1997); enCIFer (Allen, 2004); PLATON (Spek, 2003).

the *tert*-butyl groups, indicating that both ligands are equivalent. The NMR spectra of **2a**, the complex *RR*-$InL_2(OAr)$ made from *R*-HL, are shown in the Supporting Information (Figure SI 2). As above, comparison of the sets of spectra for **2** and **2a** show that approximately 90% of compound **2** is homochiral (a mixture of *RR*- and *SS*-$InL_2(OAr)$).

A reaction between InN''_3 and 3 equiv of HL at 80 °C for seven days afforded the complex *rac*-InL_3 **3** after workup (eq 3).

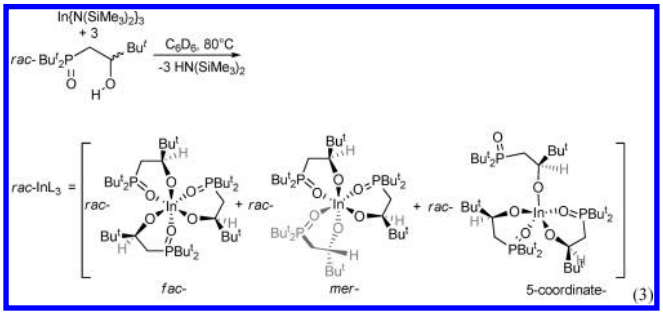

The NMR spectra of solutions of analytically pure **3** in benzene-d_6 at room temperature display multiple resonances in the *tert*-butyl region of the ^{1}H NMR spectrum and in the ^{31}P NMR spectrum, indicating that a mixture of compounds with different arrangements of the three ligands around the metal is present. It is assumed that some of these will be the five-coordinate form of InL_3 in which one phosphine oxide group remains uncoordinated. A variety of NMR spectroscopic experiments (1D and 2D, ^{1}H and ^{31}P) are included in the Supporting Information, sections 1 and 2, Figures SI 3−12.

A variable-temperature ^{1}H and ^{31}P NMR spectroscopic study of **3** in toluene-d_8 was undertaken. A stackplot showing the variation with temperature of the $^{31}P\{^1H\}$ NMR spectra of *rac*-InL_3 (**3**) are shown in the Supporting Information (Figure SI4). At low temperatures (238 K), the $^{31}P\{^1H\}$ NMR spectrum shows four sharp resonances in the region 65−70 ppm (with an integration ratio of 3:3:2:3). At 298 K, they have collapsed to three resonances with an integration ratio of 6:2:3, which remains essentially unchanged up to 338 K. This confirms the presence of different geometric isomers. The lower-frequency resonance (65.5 ppm) is tentatively assigned as the pendant PO group of a monodentate ligand. So far, we were unsuccessful in obtaining ^{115}In NMR spectra of solutions of **3**, possibly due to its fluxional behavior and high quadrupole moment of indium ($I = 9/2$).

The FTIR spectra in the solid state and solution are more informative than the NMR spectra of **3**, since it is possible to see both a coordinated P═O (1106 cm^{-1}) and

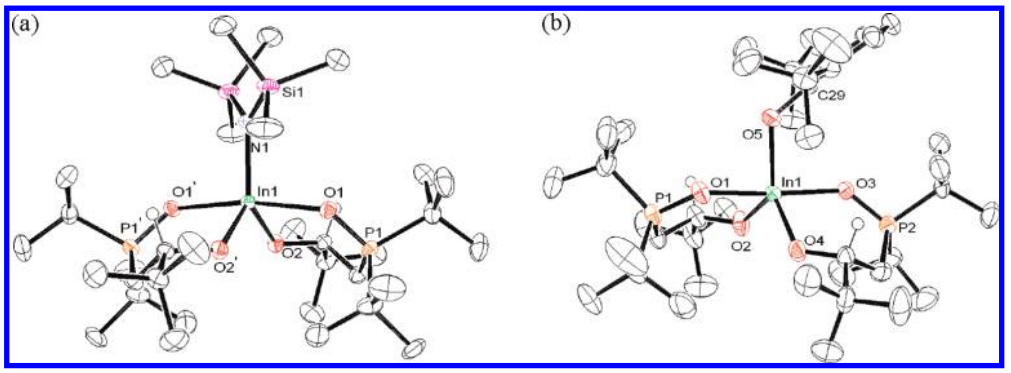

Figure 1. Displacement ellipsoid drawing of **1** (a) and **2** (b) 50% probability ellipsoids. All hydrogen atoms except the chiral CH group are omitted. Selected distances (Å) and angles (deg) for **1**: In1−O2, 2.0604(13); In1−O1, 2.2337(13); In1−N1, 2.101(2); O1−In1−O1′, 170.38(7); O2−In1−O2′, 111.40(8); O1−In1−N1, 94.81(4); O2−In1−N1, 124.30(4); O2−In−O1, 86.50(5). Selected distances (Å) and angles (deg) for **2**: In1−O1, 2.193(2); In1−O2, 2.037(2); In1−O5, 2.072(2); O3−In1−O1, 173.29(10); O2−In1−O4, 107.75(13); O4−In1−O5, 132.14(12); O5−In1−O2, 119.67(12); C29−O5−In1, 129.3(2).

uncoordinated P═O (1065 cm^{-1}) in the solid-state spectrum (nujol mull) or alternatively a coordinated P═O (1107 cm^{-1}) and uncoordinated P═O (1077 cm^{-1}) in solution (noncoordinating toluene solution).

Thus, although the bulk composition and purity of **3** has been confirmed, the number of species and identification of the range of structures of the compounds present in the bulk has not been possible. Different batches of single crystals have been structurally analyzed to provide further insight (vide infra). However, considering that one ligand is lost upon initiation of lactide polymerization, it seemed reasonable to study the utility of **3** as a polymerization initiator in spite of our incomplete understanding of its solution structure.

3.2. Crystal Structures of Complexes 1−3. 3.2.1. Crystals Structures of Complexes 1 and 2. Colorless crystals of complexes **1** and **2** suitable for a single-crystal X-ray diffraction study were grown from a hexanes solution and a DME solution, respectively. The molecular structures are depicted in Figure 1. The configuration of the molecules shown is In(*R*-L)$_2$N″ for **1** and In(*S*-L)$_2$(OAr) for **2**. The homochirality is crystallographically imposed by 2-fold rotational symmetry for **1**. In both crystals, the other enantiomer is also present in the same crystal.

The metal center in each complex shows a distorted trigonal bipyramidal geometry, with the sterically demanding (Bu^t)$_2$PO groups opposite each other in axial sites. The apical group (amido in **1** and aryloxo in **2**) occupies one equatorial site, the other two being occupied by the alkoxide groups of the ligand. The O−In−O angle formed by the two phosphine oxide ligating groups is close to linear in both (O1−In−O1′ = 170.38° for **1**, O3−In−O1 = 173.29° for **2**).

The apical group and the two alkoxide oxygens form a trigonal plane in each complex, with angles close to 120° (O2−In−O2′ = 111.40, O2−In−N1 = 124.30° for **1**, O2−In−O4 = 107.75°, O4−In−O5 = 132.14°, O5−In−O2 = 119.67° for **2**). The aryloxide ligand is bent by a very large angle (C29−O5−In1: 129.3(2)°). Space filling plots that show how the large amido and aryloxo ligands in the two crystals help the ligand self-recognition of the two L ligands are contained in the Supporting Information (Figure SI 13).

3.2.2. Crystal Structure of *rac*-InL$_3$, 3. Three different batches of crystals of **3** suitable for a single-crystal X-ray diffraction study were isolated from concentrated DME solution or a mixture of hexane and DME solution, two afforded *mer*-*RRR*-InL$_3$ and one afforded *fac*-*RRR*-InL$_3$. Figure 2 contains drawings of the two different molecular structures.

The C_3-symmetric, octahedrally coordinated *RRR*-InL$_3$/*SSS*-InL$_3$ was observed for complex **3** (Figure 3a). This is the same structure as was found by spectroscopic and X-ray diffraction analyses for the lanthanide analogs with a fac ligand arrangement. However, in **3′**, one of the ligands points in the opposite direction, b in Figure 3, forming a homochiral octahedral complex with a mer ligand conformation.[46]

Interestingly, the only significant difference in the coordinated ligand geometries is that In−OP in the mer ligand is longer than the two other In−OP bond lengths (compare In−O5 = 2.3333 Å with In−O1 = 2.2768 Å and In1−O3 = 2.2707 Å). This is shown in Table 2, and highlighted visually in a space-filling plot, in comparison with YL$_3$ (see Supporting Information, Figure SI 14).

From the above data on **3**, we conclude that, even in the compound made from enantiopure ligands, there are at least three isomers present in the solid state and in solution: fac, mer, and a five-coordinate InL$_3$ isomer with a free PO (presumably five-coordinate and not dimeric).

3.3. Polymerization of *L*- and *rac*-Lactide Using Complexes 1, 2, and 3. 3.3.1. *L*- and *rac*-Lactide Polymerization Using *rac*-InL$_2$N″, 1. First, *rac*-InL$_2$N″ (**1**) was tested as an initiator for the polymerization of *rac*-lactide (eq 4). A solution of **1** was added to a solution of *rac*-lactide; the polymerization conditions and results are collated in Table 3.

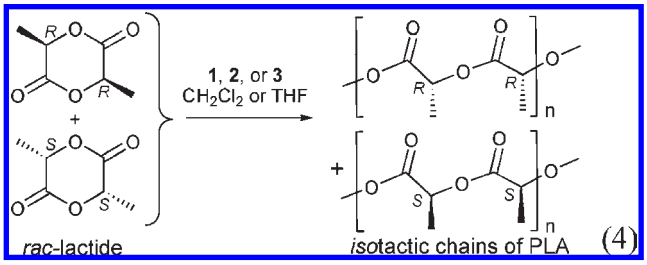

At room temperature, with a monomer/catalyst/solvent ratio of 1108:1:11000, entry 6, the polymerization is

(46) Herrero, S.; Uson, M. A. *Dalton Trans.* **2008**, 4993–4998.

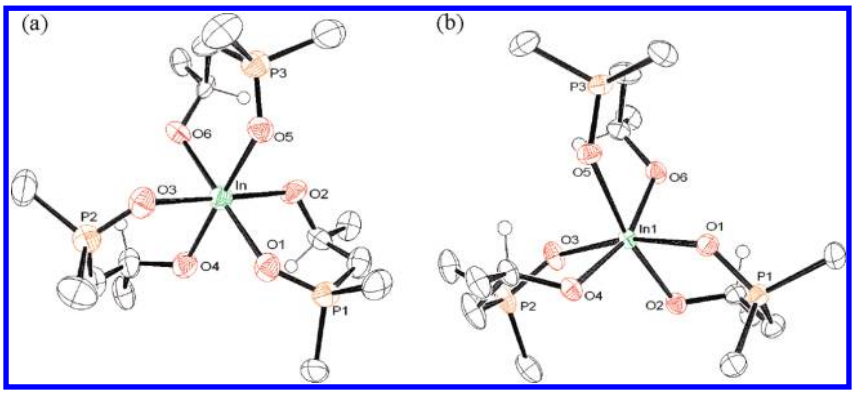

Figure 2. Displacement ellipsoid drawings of *rac*-InL_3, **3**, in the homochiral form *fac-RRR*-InL_3 (a) and *mer-RRR*-InL_3 **3′** (b), 50% probability ellipsoids. The *tert*-butyl groups and all hydrogen atoms except those at the chiral carbon atoms are omitted. Selected distances (Å) and angles (deg) for **3**: In1−O5, 2.268(9); In1−O3, 2.274(9); In1−O1, 2.265(9); O3−In1−O1, 89.9(3); O6−In1−O2, 99.1(3); O2−In1−O4, 101.1(4); O4−In1−O5, 169.1(4); O5−In1−O6, 85.7(3). Selected distances (Å) and angles (deg) for **3′**: In1−O5, 2.3333(16); In1−O3, 2.2707(17); In1−O1, 2.2768(16); O3−In1−O1, 166.24(6); O6−In1−O2, 95.68(7); O2−In1−O4, 102.65(7); O4−In1−O5, 83.20(6); O5−In1−O6, 80.24(6).

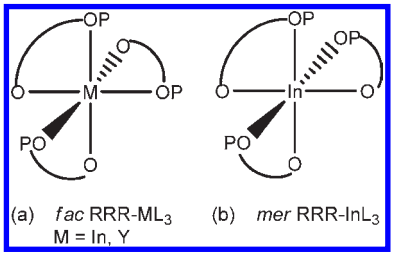

Figure 3. Drawing of molecular structures identified by crystallography for (a) *rac*-ML_3 with the ligands in the C_3-symmetric conformation and fac configuration, M = In, Y, and (b) *rac*-InL_3 with a mer ligand and mer configuration.

slow; a conversion of 26% is attained after 8 h, the molecular weight is high (39 500 g/mol), and the PDI good (1.11). Entries 2−6 show the linear relationship between M_n and increasing monomer conversion (plotted in Supporting Information Figure SI 15) and the good correlation of the theoretical molecular weight, calculated assuming that the polymer chain growth occurs from a single ligand site at the metal at low conversion. The PDI remains low until 56% conversion, entry 7, by which point it has increased to 1.26. It is also important to notice that M_n is lower in entry 7 than in entry 6 due to the onset of competing transesterification reactions. The use of dichloromethane rather than THF as the solvent for the polymerization reaction increases the rate; full conversion is attained after 16 h with $M_{n,exp}$, of 120 500 g/mol, and a PDI of 1.56, entry 8. Compared with the indium initiator reported by Mehrkhodavandi et al.,[28] the polylactide polymers made here have similar PDI values (around 1.1−1.5) and polymer molecular weights (from 20 000 to 40 000 g/mol). Mass spectral analysis of the polymer indicates that each chain is terminated by a $-N(SiMe_3)_2$ group in this case (see the Supporting Information, section 4.1). For comparison, InN''_3 showed no initiation of *rac*-lactide in CH_2Cl_2 (83:1:70 000 monomer/initiator/solvent) at room temperature after 16 h (Supporting Information, section 4.5).

The influence of the stereochemical purity of the catalyst was also investigated in the polymerization of *L*-lactide by *rac*-InL_2N'' (**1**) and *RR*-InL_2N'' (**1a**). Complex **1** polymerizes *L*-lactide (*SS*-lactide) more slowly than **1a**, demonstrating that the *RR*- form favors the insertion of the *L*-lactide and thus shows faster and better controlled polymerization of *L*-lactide. As shown in Table 4, entries 12 and 13, the PDI of polymer made by **1** of 2.81 is compared to **1a** with 1.13. It appears that the *SS*-InL2N″ also present is still reactive, but not to generate the polymer at an appreciable rate. It may be that it catalyzes transesterification more readily in the absence of a fast polymerization, decreasing the quality (molecular weight and PDI) of the polymer already formed.[32]

3.3.2. Polymerization *rac*-Lactide Initiated by *rac*-InL_2(OAr) 2 and *rac*-InL_3 3. The data from a series of polymerizations of *rac*-lactide by **2** and **3** in dichloromethane solution are collated in Table 5.

At room temperature, with a monomer/catalyst ratio of 1248:1, full conversion is attained after 16 h to afford a polymer with an $M_{n,exp}$ of 236 000 g/mol, an $M_{n,theo}$ of 174 467 g/mol, and a PDI of 1.28 (Table 5, entry 22).

The polymerization is slightly slower with a monomer/catalyst ratio of 2496:1; a conversion of 78% is attained after 16 h to afford a polymer with an $M_{n,exp}$ of 243 000 g/mol, an $M_{n,theo}$ of 280 474 g/mol, and a PDI of 1.43 (entry 23).

The GPC chromatogram traces show shoulders on the main peaks at low conversion (Table 5, entries 17−19), but these disappear at high conversion (Table 5, entries 20−22).

The molecular weights follow a linear relationship to monomer conversion. This dependence, and the low polydispersities measured, indicate the controlled propagation characteristics of these polymerizations.

Figure 4 contains the GPC chromatogram traces for a selection of the polymerization reactions of *rac*-lactide by *rac*-InL_3 (**3**). The series show how the experimental molecular weight increases with an increasing monomer/catalyst ratio, 624:1 ($M_{n,exp}$ of 120 500 g/mol), 1248:1 ($M_{n,exp}$ of 236 000 g/mol), and 2496:1 ($M_{n,exp}$ of 282 500 g/mol; Table 5, entry 16, 22 and 24, Figure 4a), and how it depends on the nature of the initiator.

The influence of the initiating group on the polymerization was investigated. Mass spectral analysis of the polymer indicates that each chain of polymer is terminated by a $-N(SiMe_3)_2$, −(OAr), or −L group for **1**, **2**, or **3**, respectively, as was also observed for the initiators YL_3

Table 2. Metal Oxygen Distances in *rac*-InL_3, **3**, and the mer Ligand Structure **3′**

distances (Å), angles (deg)	"fac ligand" **3′**	"fac ligand" **3′**	"mer ligand' **3′**	"fac ligand" **3**	"fac ligand" **3**	"fac ligand" **3**
In−OP	2.2768(16)	2.2707(17)	2.3333(16)	2.268(9)	2.274(9)	2.265(9)
In−OR	2.0864(16)	2.0656(16)	2.0611(16)	2.077(9)	2.073(9)	2.074(9)
O−P	1.5106(17)	1.5120(18)	1.5084(17)	1.487(10)	1.512(10)	1.499(10)
O−R	1.385(3)	1.393(3)	1.399(3)	1.366(17)	1.400(17)	1.411(16)
P−C	1.816(3)	1.816(3)	1.805(3)	1.802(14)	1.820(15)	1.819(15)
C−C	1.556(3)	1.552(3)	1.551(3)	1.572(18)	1.46(2)	1.51(2)
P−C1−C2−O	−61.9 (2)	−57.9 (3)	−65.6 (3)	68.3(13)	65.0(15)	67.9(13)

Table 3. Polymerization of *rac*-Lactide by *rac*-InL_2N'', **1**

entry	cat/monomer/solvent ratio (mol %)	T (°C)	time (h)	conv.[a] (%)	$M_{n,exp}$[b,c] (g/mol)	$M_{n,th}$[d] (g/mol)	M_w/M_n[e]	P_m[c]
1	1:554:11000[f]	25	16	95	64000	76727	1.63	
2	1:1108:11000[f]	25	1	7	5000	11 509	1.08	
3	1:1108:11000[f]	25	2	14	19000	23498	1.18	atactic
4	1:1108:11000[f]	25	4	20	28000	32929	1.12	0.39
5	1:1108:11000[f]	25	6	25	34500	41081	1.10	0.37
6	1:1108:11000[f]	25	8	26	39500	42679	1.11	0.37
7	1:1108:11000[f]	25	24	56	38000	90314	1.26	atactic
8	1:1108:9400[g]	25	16	>99	120500	159049	1.56	0.35
9	1:1108:94000[g]	25	16	25	37000	41081	1.96	atactic
10	1:1108:94000[g]	25	24	28	81000	45077	1.48	atactic
11	1:1108:94000[g]	25	48	52	46500	83601	1.87	

[a] Conversion of LA monomer $\{([LA]_0 - [LA])/[LA]_0\}$. [b] Measured by GPC, values based on polystyrene standards, weight corrected by multiplication by 0.58 [Mark−Houwink equation]. [c] The probability of forming a new isotactic dyad (assuming negligible transesterification), determined by ^{1}H NMR spectroscopy. [d] Molecular weight theoretical calculated using M_{th} = conv. × $[mono]_0/[cat]_0 \times M_{Mono}$. [e] Polydispersity index (M_w/M_n), PDI, measured by GPC. [f] Solvent = tetrahydrofuran. [g] Solvent = CH_2Cl_2.

Table 4. Comparison of Polymerization of *L*-Lactide Using *rac*-InL_2N'', **1**, and *RR*-InL_2N'', **1a**

entry	cat/monomer/solvent ratio (mol %)	initiator	T (°C)	time (h)	conv.[a] (%)	$M_{n,exp}$[b,c] (g/mol)	$M_{n,th}$[d] (g/mol)	M_w/M_n[e]	P_m[c]
12	1:554:9400[f]	*rac*-InL_2N''	25	16	91	26500	73290	2.81	0.37
13	1:554:9400[f]	*RR*-InL_2N''	25	16	>99	63500	90011	1.13	0.99

[a] Conversion of LA monomer $\{([LA]_0 - [LA])/[LA]_0\}$. [b] Measured by GPC, values based on polystyrene standards, weight corrected by multiplication by 0.58 [Mark−Houwink equation]. [c] The probability of forming a new isotactic dyad (assuming negligible transesterification), determined by ^{1}H NMR spectroscopy. [d] Molecular weight theoretical calculated using M_{th} = conv. × $[mono]_0/[cat]_0 \times M_{mono}$. [e] Polydispersity index (M_w/M_n), PDI, measured by GPC. [f] Solvent = CH_2Cl_2;.

Table 5. Polymerization Data of *rac*-$InL_2(OAr)$, **2**, and *rac*-InL_3, **3**

entry	cat.	cat/monomer/solvent ratio (mol %)	T (°C)	time (h)	conv.[a] (%)	$M_{n,exp}$[b,c] (g/mol)	$M_{n,th}$[d] (g/mol)	M_w/M_n[e]	P_m[c]
14	3	1:624:6200[f]	25	16	95	44500	86508	2.08	-
15	3	1:624:110000[g]	25	2.5	56	51000	50913	1.66	0.63
16	3	1:624:110000[g]	25	16	83	120500	75893	1.25	0.52
17	3	1:1248:110000[g]	25	0.17	2				
18	3	1:1248:110000[g]	25	0.5	9	26500	16594	1.46	0.30
19	3	1:1248:110000[g]	25	1	21	39500	39501	1.23	atactic
20	3	1:1248:110000[g]	25	4	42	139000	76115	1.28	0.44
21	3	1:1248:110000[g]	25	8	45	147000	81706	1.30	0.47
22	3	1:1248:110000[g]	25	16	99	236000	174467	1.28	0.54
23	3	1:2496:110000[g]	25	16	78	243 000	280474	1.43	
24	3	1:2496:110000[g]	25	40	91	282500	332420	1.43	0.36
25[e]	2	1:1170:100000[g]	25	16	42	105000	71169	1.66	0.38

[a] Conversion of LA monomer $\{([LA]_0 - [LA])/[LA]_0\}$. [b] Measured by GPC, values based on polystyrene standards, weight corrected by multiplication by 0.58 [Mark−Houwink equation]. [c] The probability of forming a new isotactic dyad (assuming negligible transesterification), determined by ^{1}H NMR spectroscopy. [d] Theoretical molecular weight calculated using M_{th} = conv. × $[mono]_0/[cat]_0 \times M_{mono}$. [e] Polydispersity index (M_w/M_n), PDI, measured by GPC. [f] Solvent = THF. [g] Solvent = CH_2Cl_2.

and YL_2N''. At room temperature, with a monomer/catalyst ratio of around 1200:1, the polymerization is faster and shows the best control with **3** (99% conversion, $M_{n,exp}$ of 236 000 g/mol, PDI of 1.28) and then with **2** (42.1% conversion, $M_{n,exp}$ of 105 000 g/mol, PDI of 1.66); and finally, **1** is the poorest (25% conversion, $M_{n,exp}$ of 37 000 g/mol, PDI of 1.96). These observed data correlate well with the expected rate of insertion of the initial lactide monomer being faster into a metal-alkoxo, followed by aryloxo, and finally an amido bond, see also the data in Figure 4b.[47−49]

(47) Cheng, M.; Attygalle, A. B.; Lobkovsky, E. B.; Coates, G. W. *J. Am. Chem. Soc.* **1999**, *121*, 11583–11584.
(48) Chisholm, M. H.; Gallucci, J.; Phomphrai, K. *Inorg. Chem.* **2002**, *41*, 2785–2794.
(49) Chisholm, M. H.; Gallucci, J. C.; Phomphrai, K. *Inorg. Chem.* **2004**, *43*, 6717–6725.

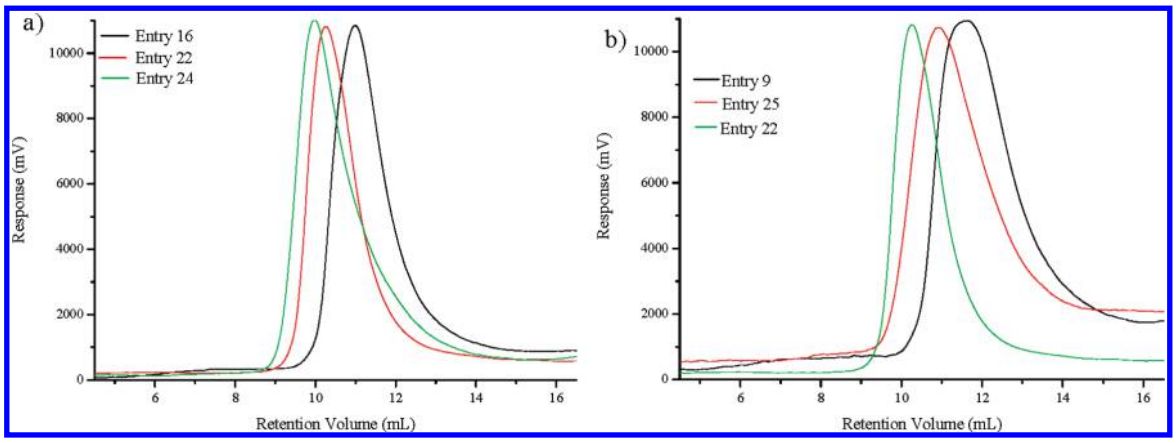

Figure 4. For the polymerization of *rac*-lactide. (a) GPC chromatogram traces for monomer/catalyst ratios of 624:1, 1248:1, and 2496:1 according to Table entry. (b) GPC chromatogram traces for the polymerization of *rac*-lactide using **1**, **2**, and **3** with monomer/catalyst ratios of 1:1108, 1:1170, and 1:1248, respectively.

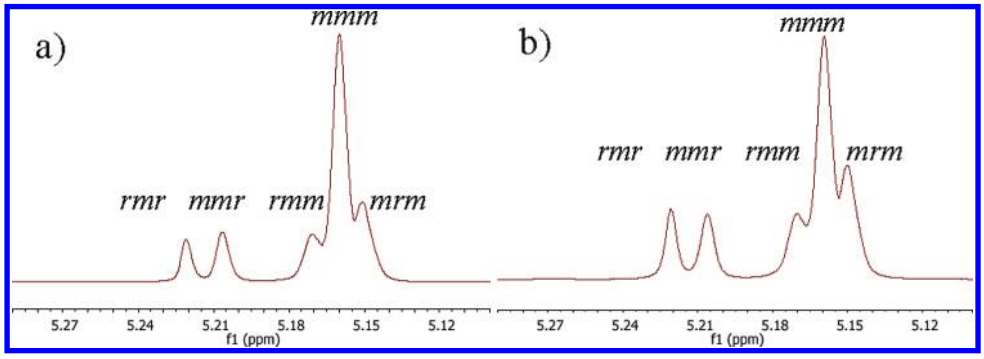

Figure 5. Methine region of homonuclear decoupled ^{1}H NMR spectra of a) isotactic PLA (Table 5, entry 15) b) isotactic PLA (Table 5, Entry 22) with assigned tetrad resonances arising from insertion errors.

Thus, **3** is behaving as a predominantly five-coordinate species in solution, or the sixth (PO) arm is particularly labile in this complex, observations backed up by the NMR and FTIR spectroscopic studies above.

Determination of the stereochemical microstructure of the PLA was achieved through inspection of the methine region of homonuclear decoupled ^{1}H NMR spectra of the resultant polymers (Figure 5). These polymers display a reasonable degree of isotacticity, which is desirable for the formation of higher melting stereocomplexes from lactide polymers.[50,51] Analysis of the ^{1}H NMR spectra of the polymers shows the *mmm* tetrad resonance for the C*H*Me proton on the polymer backbone to comprise 50 to 63% of the chemically inequivalent methine resonances (Figure 5a, *mmm* tetrad of 63%, entry 15 and Figure 5b, *mmm* tetrad of 53%, entry 22). This demonstrates a significant amount of isotactic polymer. The presence of insertion defects in the polymer gives rise to a smaller set of methine resonances due to presence of *mmr*:*mrm*:*rmr*:*rmm* arrangements of the chiral centers. The ratio of these defect resonances is 1:2:1:1, which are caused by single insertion defects (e.g., polymer microstructures of $-RRRRRRSSRRRRRR-$ (and vice versa)) rather than the formation of a stereoblock polymer (where the defects would be due to a polymer microstructure of $-RRRRRRSSSSSS-$ (and vice versa)).

(50) Fan, Y.; Nishida, H.; Shirai, Y.; Tokiwa, Y.; Endo, T. *Polym. Degrad. Stab.* **2004**, *86*, 197–208.
(51) Zhang, J.; Tashiro, K.; Tsuji, H.; Domb, A. J. *Macromolecules* **2007**, *40*(4), 1049–1054.

4. Conclusion

We have synthesized a series of five- and six-coordinate indium complexes derived from chiral $(^t\text{Bu})_2\text{P(O)CH}_2\text{CH}(^t\text{Bu})$-OH. Their catalytic behavior in the ROP of *rac*-lactide polymerization varies remarkably. Complex *rac*-InL_3 (**3**) had the highest activity and stereoselectivity among all complexes, despite the spectroscopic data, suggesting that it is not a configurationally well-defined complex. We suggest that if complex **3** is mostly present in solution as a homochiral, but only as five-coordinate species, then the third, monodentate ligand L may act as an initiating alkoxide group for chain end control. This still leaves a chiral pocket at the metal generated by the two remaining L's, which helps to control further insertions of chiral lactide monomers. Studies of the polymerization of other biorenewable monomers by these complexes are in progress.

Acknowledgment. This work was supported by the University of Edinburgh, EaStCHEM, and the Moray Endowment Fund. We thank Prof. Mark Bradley (University of Edinburgh) for the use of Gel Permeation Chromatography and Prof. Simon Parsons for the use of the diffractometer.

Supporting Information Available: Additional graphs and data and crystallographic data (CIF format) for complexes **1**, **2**, **3**, and **3′** (CCDC codes 727821−727824, also available on request from the Cambridge crystallographic database http://www.ccdc.cam.ac.uk/). This material is available free of charge via the Internet at http://pubs.acs.org.